Proceedings of the IASS 2024 Symposium
Redefining the Art of Structural Design
August 26-30, 2024, Zurich, Switzerland
Philippe Block, Giulia Boller, Catherine DeWolf,
Jacqueline Pauli, Walter Kaufmann (eds.)

Plotting Eccentricity Lines on continuous shells: discussion and examples

Arianna VENETTONI*, Valerio VARANO*, Ginevra SALERNO*, Stefano GABRIELE*

* Roma Tre University
Via Aldo Manuzio, 72, 00153 Rome, Italy
arianna.venettoni@uniroma3.it

Abstract

Several families of lines can be generated on a curved surface by plotting different properties. These lines can be classified as either geometrical, or strictly mechanical if the surface becomes a shell structure. A great deal of previous research about mechanical streamlines has focused on plotting principal stress lines and select the most meaningful for the definition of a gridshell layout. Here, we introduce a new typology of mechanical lines: the eccentricity lines, based on the principle of R-Funicularity; in this work we assess the significance of the generalized eccentricity as a synthesis of principal stress and bending moments. Even though there is softwares available that currently plots the principal lines, several integration issues can occur that reflect in drawing the lines. Furthermore, the plotting of eccentricity lines may face additional difficulties due to singularity points that, for example, emerge when the eigenvalue problem associated to the eccentricity tensor is ill-posed. This study proposes an algorithm for the regularization and the plotting of eccentricity lines on continuous shells using Grasshopper and Karamba 3D. The effectiveness of the proposed method will be then demonstrated through the analysis of several examples of significant shell structures.

Keywords: streamlines, generalized eccentricity, shell structure, R-Funicularity

1. Introduction

The shape of a shell has a greater impact on its structural behavior than any other aspect; as a result, several form finding methods have been created and implemented in order to determine the ”optimal” structural geometry in static equilibrium with a certain load pattern [1]. Despite efforts to connect the concepts of form and structure, today’s construction process typically maintains a strict distinction between architecture and engineering. In the perspective of overcoming this obstacle, lines that illustrates the principal directions of forces might be viewed as a helpful tool to assist designers in visualizing and understanding the flow of forces through any continuous shell.

The visualization of force flow on shells is becoming a significant topic in architectural, engineering, and applied geometry domains, as evidenced by several research. This topic is strictly connected to the challenge of identifying structures subjected to specific loads with minimal volume while stress levels do not exceed imposed limits. Nevertheless, the research to date has tended to focus on the plotting of the *principal stress lines*, attempting to produce optimal solutions for gridshells or ribbed slabs [2], [3], [4]; thus, most of the recent findings can only be applied to membrane shell structures. Bending moments, regardless how small, will always occur when designing and actual surface, and this applies as well to form found shells, as thickness increases and the ratio between membrane and flexural stiffness decrease. It is then useful to examine the combined effects of principal membranes forces and bending moments; therefore, this research focuses on the analysis and the plotting of principal eccentricity lines.

This topic is strictly linked to the recent definition of Relaxed Funicularity and the analysis of the principal directions of eccentricity, introduced by some of the authors in [5]. The purpose of this paper is to deepen the understanding of these topic by exploring the definition and visualization of the eccentricity lines fields, as well as providing an actual numerical example of their generation.

2. Theoretical background

2.1. Principal Modulus Eccentricity directions

The concept of Relaxed Funicularity (also known as R-Funicularity or RF), extends the notion of funicularity for continuous shells. The RF was developed to assess the shape quality of a shell under specific load and boundary condition cases, taking into account the effects of "small" moments. Determining a generalized eccentricity (GE) measure and ensuring that it falls within certain eccentricity limits allows for the quantification of RF.

The generalized eccentricity is defined as the ratio between the generalized bending moment and the generalized membrane force:

$$e(\theta) = \frac{M(\theta)}{N(\theta)} = \frac{\mathbf{u}^T \mathbf{M} \mathbf{u}}{\mathbf{u}^T \mathbf{N} \mathbf{u}} \tag{1}$$

Then, for each point of the shell, the GE is a function of θ, which is the angle between the unit vector $\mathbf{u} = (\cos(\theta), \sin(\theta))$ and the base vector $\mathbf{e}_1$. In [6] it has been proved that, because equation (1) is a Rayleigh quotient, the maximum and minimum eccentricities (e_{max}, e_{min}) can be found by solving the following generalized eigenvalue problem $(\mathbf{M} - e\mathbf{N})\,\mathbf{u} = 0$.

Provided that $\mathbf{N}$ is invertible, the local extrema e_{max} and e_{min} can be calculated as eigenvalues of what we can call *Eccentricity Tensor* $\mathbf{E} = \mathbf{N}^{-1}\mathbf{M}$.

The solution is the following:

$$e_{\text{min}} = \frac{1}{2}\left(E_{11} + E_{22} - \sqrt{(E_{11} + E_{22})^2 - 4E_{12}E_{21}}\right) \tag{2.1}$$

$$e_{\text{max}} = \frac{1}{2}\left(E_{11} + E_{22} + \sqrt{(E_{11} + E_{22})^2 - 4E_{12}E_{21}}\right) \tag{2.2}$$

It is important to underline that, although $\mathbf{N}$ and $\mathbf{M}$ are symmetric, in general the tensor $\mathbf{E}$ is non-symmetric, unless $\mathbf{N}$ and $\mathbf{M}$ commute. There are two key differences between the eigenvalue problem for non-symmetric and symmetric tensors: the eigenvalues of a non-symmetric tensor can assume complex values and, in general, the eigenvectors of a non-symmetric tensor are not perpendicular to each other.

These differences can create several issues in the process of defining and representing the Principal Eccentricity (PE) vectors. In order to fix these problems, the authors believe it is more helpful to define the principal eccentricity directions using the angle values θ_{min} and θ_{max}.

$$\theta_{\text{min}} = \frac{1}{2}\left[\arctan\left(\frac{E_{12}+E_{21}}{E_{11}-E_{22}}\right) - \arctan\left(\frac{\sqrt{4E_{12}E_{21}+(E_{11}-E_{22})^2}}{E_{12}-E_{21}}\right) - \frac{\pi}{2}\right] \tag{3.1}$$

$$\theta_{\text{max}} = \frac{1}{2}\left[\arctan\left(\frac{E_{12}+E_{21}}{E_{11}-E_{22}}\right) + \arctan\left(\frac{\sqrt{4E_{12}E_{21}+(E_{11}-E_{22})^2}}{E_{12}-E_{21}}\right) - \frac{\pi}{2}\right] \tag{3.2}$$

In contrast to the mechanical meaning of the sign of $N(\theta)$ (tension vs compression), the sign of $M(\theta)$ is entirely conventional. Therefore, the sign of $e(\theta)$, which determines whether the shell stresses' resultant is located above or below the shell's middle surface, is irrelevant when measuring the R-Funicularity. The authors reckon that the Modulus Eccentricity (ME:=$|e(\theta)|$) is a more significant parameter.

The concept of maximum Modulus Eccentricity (ME) has been introduced in [6], and also applied to shell's shape optimization in [7]. In this paper we choose to define both the maximum and minimum ME directions, and we use them to plot the correct principal ME Lines.

Here we summarize the general criteria we followed to determine the right directions. If we define:

$$\text{E}_{\text{min}}, \text{E}_{\text{max}} = \min(|e(\theta)|), \max(|e(\theta)|) \tag{4}$$

$$\Theta_{\text{min}}, \Theta_{\text{max}} = \underset{\theta}{\text{argmin}}\,(|e(\theta)|), \underset{\theta}{\text{argmax}}\,(|e(\theta)|) \tag{5}$$

the solution is:

$$\text{E}_{\text{min}}, \Theta_{\text{min}} = \begin{cases} |e_{\text{min}}|, \theta_{\text{min}} & if\ \det(\mathbf{N}) > 0\,\&\,|e_{\text{max}}| \geq |e_{\text{min}}| \\ |e_{\text{max}}|, \theta_{\text{max}} & if\ \det(\mathbf{N}) > 0\,\&\,|e_{\text{max}}| < |e_{\text{min}}| \\ 0, \theta_0 & if\ \det(\mathbf{N}) \leq 0 \end{cases} \tag{6}$$

$$\text{E}_{\text{max}}, \Theta_{\text{max}} = \begin{cases} |e_{\text{max}}|, \theta_{\text{max}} & if\ \det(\mathbf{M}) > 0\,\&\,|e_{\text{max}}| \geq |e_{\text{min}}| \\ |e_{\text{min}}|, \theta_{\text{min}} & if\ \det(\mathbf{M}) > 0\,\&\,|e_{\text{max}}| < |e_{\text{min}}| \\ \infty, \theta_\infty & if\ \det(\mathbf{M}) \leq 0 \end{cases} \tag{7}$$

where:

$$\theta_0 = \beta_M \pm \frac{1}{2}\arccos\left(\frac{-\text{Tr}(\mathbf{M})}{\Delta M}\right) \tag{8}$$

$$\theta_\infty = \beta_N \pm \frac{1}{2}\arccos\left(\frac{-\text{Tr}(\mathbf{N})}{\Delta N}\right) \tag{9}$$

and $(e_{\text{min}}, e_{\text{max}}), (\theta_{\text{min}}, \theta_{\text{max}})$, are calculated by means of the equations (2.1,2.2), (3.1,3.2), respectively.

Is is fundamental to highlight that:

- If $\det(\mathbf{M}) \leq 0$, there are two different values of θ such that $e(\theta) = 0$, evaluated using equation (8). Therefore, there are two Minimum ME directions, symmetric with respect to β_M, and two corresponding values of $\Theta_{min} = \theta_0$.
- If $\det(\mathbf{N}) \leq 0$, there are two different values of θ such that $e(\theta) = \infty$, evaluated using equation (9). Therefore, there are two Maximum ME directions, symmetric with respect to β_N, and two corresponding values of Θ_{max}.

For a complete investigation of the generalized eccentricity and the ME'.s formulation, refer to the author's previous work [8] and [9].

2.2. Streamlines generation

Usually related to fluids flow, streamlines are a family of curves whose tangent vectors constitute the velocity vector field of the flow. In a structure, these lines can show the flow of different force fields by connecting the projections of principal vectors directions (namely the eigenvectors) for a collection of points across the structural body. Multiple vector fields, such as principal stress, moments, or eccentricity, can be represented.

Despite the development and application of numerous tools, the most accurate process for the generation of streamlines is still up for debate.

The streamline tracing process has to begin with a seed location for each line; then it evaluates the next line's point following the direction of the tangent vectors. The process of selecting the right seed points to generate significant streamlines is called *"seeding"*. Subsequently, the principal directions and values are estimated for the centroids of the input mesh, since the vector field to be investigated is derived from a finite element analysis; *data interpolation* must be handled in the streamlines generation process in order to compute the data for any point. The last step is the actual *integration* of the vectors to define the streamline path in both directions. The most commonly used integration methods are Euler's and Runge-Kutta's.

It is important to note that, because its directions can point both forward and backward simultaneously, a vector field resulting from a FEA analysis is not exactly the same as a conventional field. This problem becomes more challenging when principal eccentricity lines are generated, due to the two major issues mentioned in the section above: the ME vectors are not perpendicular to each other, and both the maximum and minimum directions might bifurcate, resulting in multiple principal directions.

3. Objectives and methods

The specific objective of this study is to define the Modulus Eccentricity vector field for any given shell structure, and to visualize its path by investigating the plotting of its streamlines.

In order to accomplish our goals, a script was created with Rhinoceros and Grasshopper 3D [10]; the structural analysis is performed using the Grasshopper plugin Karamba3D [11], which allows the principal directions to be evaluated. Based on the idea of visual scripting, Grasshopper enables the development of user subroutines that are adapted to the particular design context. This software is highly customizable and flexible, making it suitable for research purposes.

This study is unable to encompass the entire streamline tracing process, so the article will focus on the proper determination of the field and the investigation of the seeding phase, while the Karamba3D "User streamlines" component will be used for the integration of streamlines. The authors intend to implement the algorithm in the near future to incorporate more efficient methods of interpolation and integration.

4. Generation of Modulus Eccentricity Lines (MEL)

The outline of the proposed procedure for the generation of the ME lines is described by the flowchart in Fig. 1.

To characterize the studied design domain, perform the FEM analysis from which structural data is extracted, and develop a suitable seeding plan, it is essential to define a proper mesh topology. The use of Grasshopper allows for the definition of the surface either using a mathematical function or through a

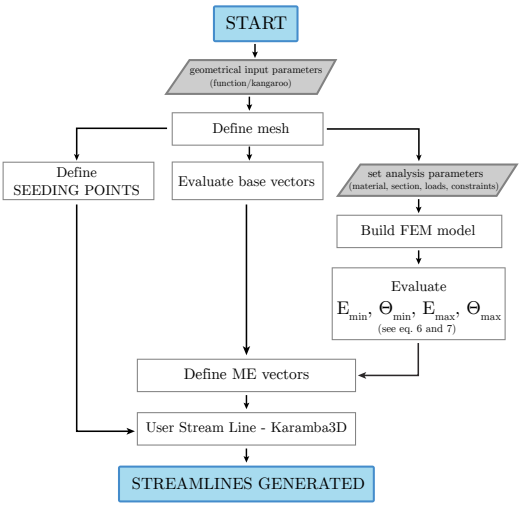

Figure 1: Flowchart of the proposed visual script.

form-finding method, employing tools such as Kangaroo; just altering the design base parameters allows for the retrieval of multiple shapes from the same script.

Once the geometry is set, it has to be converted into a triangulated mesh. It is essential to calibrate the mesh's regularity and density during this phase because the output is highly related to the quality of the triangulation, yet a high density mesh will result in a time-consuming computational procedure. The mesh is then turned into a shell by Karamba3D. Simultaneously, the surface and mesh data are stored in a separate cluster to extract the coordinate vectors $\mathbf{u}$, $\mathbf{v}$ and $\mathbf{n}$, that will be later used to generate the ME vectors. Loads, cross section and supports are then defined; the Karamba3D script assembles the model and performs the FEM analysis.

Through the "Shell forces" component, the algorithm evaluates N and M in local directions, and defines their values as N_{xx}, N_{yy}, N_{xy} and M_{xx}, M_{yy}, M_{xy}. The finite element analysis performed with Karamba3D outputs the principal stress values in every centroid point of the mesh, but the "User streamlines component" requires a vector for each node of the model; therefore, the generation of ME lines has to begin with some sort of data interpolation, which involves computing the data for every vertex of the mesh. This research uses a custom GhPython component to link each vertex with the adjacent mesh faces and average the values of the elements which connect to that node.

The algorithm assembles the $\mathbf{N}$ and $\mathbf{M}$ matrices and computes the $\mathbf{N}^{-1}\mathbf{M}$ matrix, thus defining the $\mathbf{E}$ tensor. Then, a GhPython component was developed to evaluate the maximum and minimum modulus eccentricities: the component calculates $\mathrm{E_{min}}, \mathrm{E_{max}}, \Theta_{\mathrm{min}}, \Theta_{\mathrm{max}}$ according to (6) and (7). The component's output is a list of angle values, each corresponding to a node of the model.

At this step, it is important to note that the bifurcation of the ME lines is determined by the relative doubled Θ values. Because there is currently no way to divide the lines during the integration process, four lists of angles are grouped independently for each node: two for the minimum and two for the maximum modulus eccentricity.

After evaluating the angle, the script computes the following operation to convert them into vectors:

$$\mathbf{E}_{max} = \cos\Theta_{max}\mathbf{u} + \sin\Theta_{max}\mathbf{v}_p \qquad \mathbf{E}_{min} = \cos\Theta_{min}\mathbf{u} + \sin\Theta_{min}\mathbf{v}_p$$

Being $\mathbf{u}$ the coordinate vector aligned with the global X direction and $\mathbf{v}_p = \mathbf{u} \times \mathbf{n}$.

The vectors are then normalized and used as input for the User Stream line component. A key aspect to consider at this stage is that the order of the outputted vectors corresponds to the enumeration of the mesh generated by Karamba3D, whereas the new component stores the points in an alternative sequence determined by the shell element. Therefore, the vectors need to be renumbered to match the right order; this can be achieved by using "Find similar member" component to reassign the item to a new ordered list.

4.1. Seeding

The plotting of ME lines, as for any other family of streamlines, starts from a seed point; the algorithm then estimates the movement direction from the vector field and iteratively searches for the next point. Generally, the goal of seeding is to identify a set of sources from which a uniformly spaced lines field can be built for further processing and selection. In this paper, seeding is also investigated in order to achieve a meaningful distribution of lines, highlighting the varying flow of forces.

5. Numerical examples

5.1. Shapes definition

To test the effectiveness of the proposed algorithm, this paper analyzes two kinds of forms: a parametric shape described by an analytical function, and a form-found one, defined using Kangaroo2.

The first shape was selected based on how simple it was to define and parametrize it in Grasshopper. It has additionally been examined earlier for form optimization [12], and some of the authors have also used it to assess the efficacy of objective functions derived from the ME in [13].

The following equation describes a parametric parabolic cylinder-shaped surface:

$$z = 4fx\frac{l_x - x}{l_x^2} \quad \text{with} \quad f = a_0 + a_1 y + a_2 y^2 \tag{10}$$

where we define a_0, a_1 and a_3 as:

$$a_0 = c_1 \qquad a_1 = 4\frac{c_2 - c_1}{l_y} \qquad a_2 = 4\frac{c_1 - c_2}{l_y^2}$$

We set $lx = 6m$ and $ly = 12m$ and we investigate the design space generated by adjusting the c_1 and c_2 parameters. The final surface to be analyzed was selected from the resulting set of shapes; the relative parameter values are $c_1 = 6$ and $c_2 = 3$.

A form-found process in Kangaroo2 is used to determine the second shape. The surface is generated from a square area with sides of 20 m, using a 1x1 m mesh; the anchor points are defined using the four vertices of the mesh and their two adjacent points; the rest length of the springs is equal to the lines' starting length; and each node of the mesh is loaded with a vertical upward force of intensity 1N. The form-found shape is a velaroidal shell with a maximum heigth of 8 m.

5.2. Analysis of Generalized Eccentricity

The parabolic cylinder-shaped shell is pinned on the longer sides; the constraints of the velaroidal shell coincide with the anchor points defined in Kangaroo. The material of both shells is set to concrete 25/30, with a cross-section's thickness of 5cm. A linear static analysis of the structures, subject to self-weight load and an in plan uniform vertical load of $5\frac{kN}{m^2}$, is then performed using Karamba3D.

As stated in Section 4., the **N** and **M** values and directions resulting from the FEM analysis are used to calculate the GE of the given shell structures; then, a Grasshopper cluster is utilized to plot the eccentricity distribution on the surfaces.

Both the $|E_{min}|$ and $|E_{max}|$ are plotted by the algorithm. The data was divided into three sets in order to make it more manageable: $x < \frac{h}{6}$, $\frac{h}{6} < x < \frac{h}{2}$ and $x > \frac{h}{2}$. We remark that the section can be considered R-funicular for eccentricity values less than $x < \frac{h}{6}$. A comparison between the GE values and vectors is shown for both shapes in Figures 2 and 3.

With the exception of two minor regions of the first case, where they nevertheless stay within half of the section's height, we can see from the eccentricity distribution that the minimum eccentricities entirely fall inside the mid-third of the section. As a result, it is reasonable to conclude that graphing the maximum modulus eccentricity is sufficient to determine R-Funicularity of the structure.

When comparing the results for the first shape, it becomes clear that the dark blue regions (where the eccentricity exceeds the boundaries) match precisely the locations of the vectors' field where the directions of maximum ME split. On the other hand, it can be observed that the directions of the second shell never bifurcate; this indicates that $\det(\mathbf{N}) > 0$ for each point, thus $N(\theta)$ is never equal to 0. Moreover, the areas where the vectors of minimum eccentricity bifurcate are found to be funicular; along these directions, there are indeed one or two different values of Θ such that $M(\theta) = 0 \rightarrow e(\theta) = 0$.

The current approach proves to be quite effective since it enables to directly identify the non-funicular zones and the orientations along which the structural shell must resist bending.

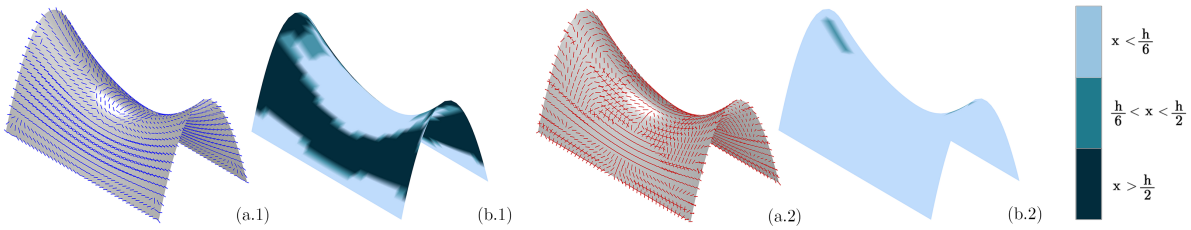

Figure 2: Results of the analytically defined shell: (a.1) $|E_{max}|$ vectors and (b.1) values; (a.2) $|E_{min}|$ vectors and (b.2) values.

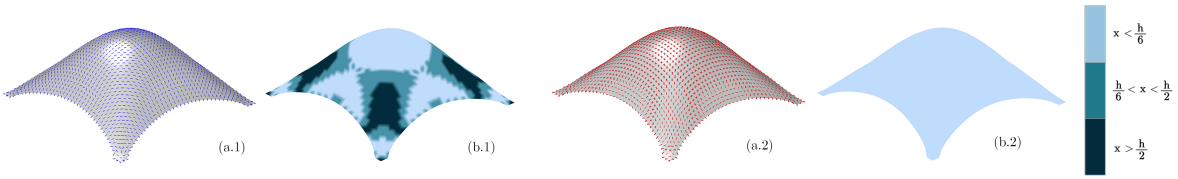

Figure 3: Results of the form-found shell: (a.1) $|E_{max}|$ vectors and (b.1) values; (a.2) $|E_{min}|$ vectors and (b.2) values.

5.3. ME lines

The ME lines network is generated through the "User stream lines" Karamba3D component, utilizing the evaluated ME vectors as inputs. Initially, an arbitrary seeding scheme is defined: the mesh vertex are extracted, culled with a random pattern and then used as seeds (Fig. 4)

Plotting the lines using Θ angles eliminates some of the issues that arise when the eigenvalue problem associated with the eccentricity tensor is not well-posed. However, the plotted lines appear confused and

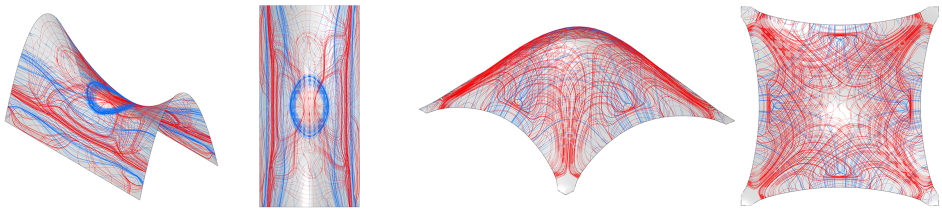

Figure 4: $|E_{min}|$ (red) and $|E_{max}|$ (blue) lines for both shell structures.

still exhibit some irregularities, such as loops, intersecting and overlapping lines.

The blackbox approach of Karamba3D tracer does not allow for meaningful intervention in the integration algorithm; hence, focusing on seeding appears to be the most effective strategy to improve the generation of the lines. The current section of the paper will thus present the investigation of several different seeding schemes. Seeding can be arbitrary or guided; arbitrary approaches might be random or dependent on other regular patterns on the input mesh, while guided methods establish a connection between the seeding strategy and meaningful numerical values [3].

As an *arbitrary* strategy, we investigate the generation of the lines using as seeds a regular grid of points based on the UV parametrization, and the surfaces' naked edges.

For the *guided* approach, we relate the seeding strategy to the mechanical properties of the structure using the shells' isolines. We use the points of: the $\Delta\beta$ isolines, being $\Delta\beta = \beta_M - \beta_N$ the relative angle between $\mathbf{M}$ and $\mathbf{N}$ eigenvectors; the $|E|$ isolines; the Gaussian curvature isolines. The tables in Fig. 5 and 6 summarize the resulting lines' layouts.

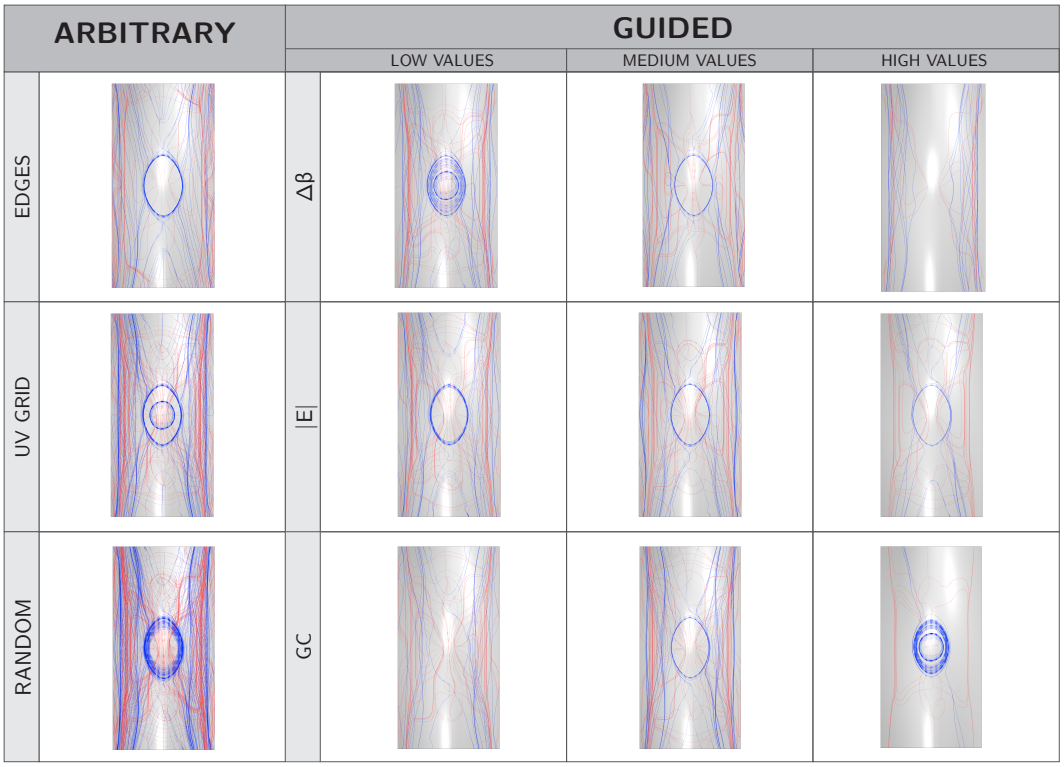

Figure 5: Seeding investigation for the analytically defined shell.

In general, relying solely on seeding analysis is not sufficient to obtain flawless lines. However, patterns

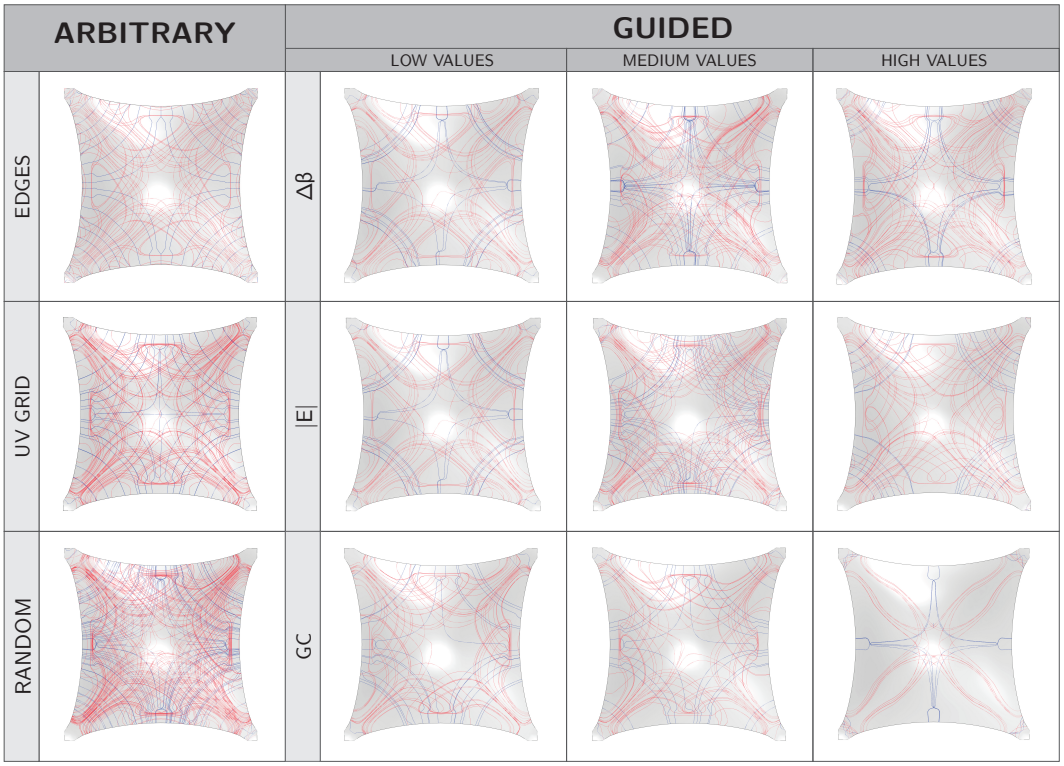

Figure 6: Seeding investigation for the form-found shell.

can be identified, especially in lines of maximum ME, which can be useful for understanding directions that may require structural reinforcement, such as concrete ribs.

The first shape's lines appear to be highly uneven in all circumstances, particularly for the minimum ME lines; this is most likely due to the surface's negative Gaussian curvature. However, it is still possible to trace a general path through the maximum ME lines: a ring stress in the center, which causes the lines to loop, and two crossing lines on the sides. The cases associated with low beta values tend to be the most clear.

The lines observed in the form-found shell generally appear more regular, owing to the shape's Gaussian curvature always positive and the membrane force never equal to zero. While the maximum ME lines may indicate the possible orientation of reinforcing ribs, the flow of the minimum ME lines may be more interesting: in fact, the locations where the lines bifurcate correspond to the points where the bending is equal to zero, allowing elements with a very small cross section to be placed along these directions. In this case, the seeding scheme that utilizes points on the edges yields the best results.

6. Conclusions

This work defined the principal eccentricity lines associated with vectors of minimum and maximum eccentricity modulus, that are useful to analyze the combined effects of principal membranes forces and bending moments. Subsequently, a method was presented to generate the ME lines on a shell using Grasshopper3D. This process utilizes Karamba3D to integrate the vectors and generate the ME lines, but the authors plan to implement it in the future to directly manage the integration phase through the script. This research then illustrated two examples of line generation, plotting them on two shells — one obtained from an analytical formula and one from a form-finding process. Finally, an analysis of seeding was presented, comparing the lines generated using different starting schemes. This investigation proved

that ME lines are interesting not only mechanically, but also aesthetically. They could therefore be used as a base scheme for inserting reinforcements or stiffening elements, as well as to define the final geometry. The goal of future research will be to further explore these possibilities.

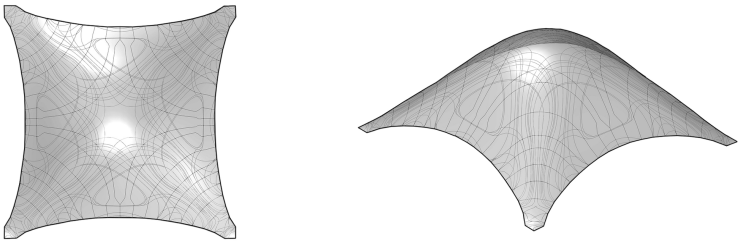

Figure 7: Example on regularized ME lines in the form found shell.

References

[1] S. Adriaenssens, P. Block, D. Veenendaal, and C. Williams, *Shell structures for architecture: form finding and optimization*. Routledge, 2014.

[2] P. Michalatos and S. Kaijima, "Eigenshells: Structural patterns on modal forms," in *Shell Structures for Architecture: Form Finding and Optimization, eds. S. Adriaenssens, P. Block, D. Veenendaal, and C. Williams*, Routledge, 2014.

[3] K. Tam and C. Mueller, "Stress line generation for structurally performative architectural design," in *Chris Perry, Lonn Combs (Eds.): 35th Annual Conference of the Association for Computer Aided Design in Architecture (ACADIA)*, 2015.

[4] M. Church, "Investigation of isostatic slab in timber," Ph.D. dissertation, Delft University of Technology, 2021.

[5] S. Gabriele, V. Varano, G. Tomasello, and D. Alfonsi, "R-funicularity of form found shell structures," *Engineering Structures*, vol. 157, pp. 157–169, 2018.

[6] M. Lucchesi, C. Padovani, G. Pasquinelli, and N. Zani, "The maximum modulus eccentricities surface for masonry vaults and limit analysis," *Mathematics and Mechanics of Solids*, vol. 4, pp. 71–88, 1999.

[7] G. R. Argento, F. Marmo, V. Varano, and S. Gabriele, "Shells' shape optimization based on r-funicularity," in *Proceedings of the IASS Annual Symposium 2020/21 and the 7th International Conference on Spatial Structures–Inspiring the Next Generation*, 2021.

[8] S. Gabriele and V. Varano, "About the directions of principal eccentricities in continuous shells," *Shell and Spatial Structures, Proceedings of IWSS 2023*, pp. 390–397, 2024.

[9] V. Varano, A. Venettoni, G. Salerno, and S. Gabriele, "Directions of eccentricity of shells: The r-funicularity perspective," to be submitted.

[10] R. McNeel *et al.*, "Rhinoceros 3d, version 7.0," *Robert McNeel & Associates, Seattle, WA*, 2010.

[11] C. Preisinger, "Linking structure and parametric geometry," *Architectural Design*, vol. 83, pp. 110–113, 2013.

[12] E. Ramm, K. Bletzinger, and R. Reitinger, "Shape optimization of shell structures," *Journal of the International Association for Shell and Spatial Structures*, vol. 34, pp. 103–121, 1993.

[13] G. R. Argento, "Shape optimization of arches and shells: An r-funicularity based approach," Ph.D. dissertation, Roma Tre University, Department of Architecture, 2024.